

Optimization of two-photon wave function in parametric down conversion by adaptive optics control of the pump radiation

M. Minozzi,¹ S. Bonora,² A. V. Sergienko,³ G. Vallone,^{1,2} and P. Villoresi^{1,2,*}

¹Department of Information Engineering, University of Padova, Padova 35131, Italy

²Institute for Photonics and Nanotechnology, National Research Council (CNR), Padova 35131, Italy

³Department of Electrical & Computer Engineering, Boston University, Boston, Massachusetts 02215, USA

*Corresponding author: paolo.villoresi@unipd.it

Received November 5, 2012; revised December 23, 2012; accepted December 23, 2012;
posted January 11, 2013 (Doc. ID 179285); published February 8, 2013

We present an efficient method for optimizing the spatial profile of entangled-photon wave function produced in a spontaneous parametric down conversion process. A deformable mirror that modifies a wavefront of a 404 nm CW diode laser pump interacting with a nonlinear β -barium borate type-I crystal effectively controls the profile of the joint biphoton function. The use of a feedback signal extracted from the biphoton coincidence rate is used to achieve the optimal wavefront shape. The optimization of the two-photon coupling into two, single spatial modes for correlated detection is used for a practical demonstration of this physical principle. © 2013 Optical Society of America
OCIS codes: 270.0270, 190.4410.

The physical idea connecting a spatial pump wavefront with the properties of generated entangled photons in the nonlinear process of spontaneous parametric down conversion (SPDC) has been studied theoretically [1,2]. Several experimental realizations have been reported by placing discrete objects such as single wire, double slits, lens, etc. [3] in the pump beam. These days, deformable mirrors (DefMs) become key devices for the modification of a laser wavefront allowing for a full control of the beam properties. DefMs have been used in several quantum optics experiments [4–6]. In this Letter we experimentally demonstrate the use of DefM technology for engineering the desired spatial profile of the entangled-photon wave function. An adaptive optics control of the pump wavefront is implemented to optimize the shape of the joint wave function of correlated two-photon pairs propagating along 2 m of free-space. In the SPDC process, pairs of photons (signal and idler) are emitted from a nonlinear crystal pumped with a laser beam. The main goal of this Letter is to demonstrate that the manipulation of the pump wavefront with a DefM could effectively control the joint spatial profile of the produced down-converted photons. In particular, we will demonstrate the optimization of diffraction characteristics in the propagation of SPDC photons.

The shape of a two-photon wave function of down-converted light naturally depends on the properties of the pump wavefront. By considering the pump beam propagating in the z direction, it is possible to show [7] that the biphoton wave function can be written as

$$|\psi\rangle = \int d^2\mathbf{k}_s d^2\mathbf{k}_i d\omega_s d\omega_i \tilde{\psi}_{\mathbf{k}_i, \mathbf{k}_s, \omega_i, \omega_s} a_{\mathbf{k}_s, \omega_s}^\dagger a_{\mathbf{k}_i, \omega_i}^\dagger |\text{vac}\rangle, \quad (1)$$

with

$$\tilde{\psi}_{\mathbf{k}_i, \mathbf{k}_s, \omega_i, \omega_s} = \mathcal{N} L A_p(\mathbf{k}_s + \mathbf{k}_i, \omega_s + \omega_i) \text{sinc}\left(\frac{L}{2} \Delta k_z\right), \quad (2)$$

where L is the crystal length, \mathbf{k}_i and \mathbf{k}_s are the transverse momentum coordinates of the signal and idler photons,

$A_p(\mathbf{k}, \omega)$ is the pump profile in the momentum-frequency space and Δk_z is the (longitudinal) phase mismatch $\Delta k_z = k_{pz} - k_{sz} - k_{iz}$. The term $\mathcal{N} = \epsilon_0 \chi^{(2)} E_p E_s E_i / (2i\hbar)$ is a function of the fields strength E . It is clear that changes in the pump profile $A_p(\mathbf{k}, \omega)$ result in the biphoton wave function modification. Therefore, a slight adjustment in the pump wavefront could lead to substantial alterations in the two-photon wave function profile that is revealed in the spatial dependence of coincidences. The usual plane wave pump produces SPDC beams that are naturally divergent in space. The goal is to use the outlined above control features for converting the divergent SPDC wavefront into a more collimated propagation profile. This task is accomplished by the use of an evolutionary feedback algorithm linking the action of the adaptive mirror with the coincidence counting rate.

The experimental setup is shown in Fig. 1. The 404 nm laser pumps a β -barium borate nonlinear crystal (NL) in order to generate SPDC photons in type-I phase matching. The waveform modulation of the pump beam

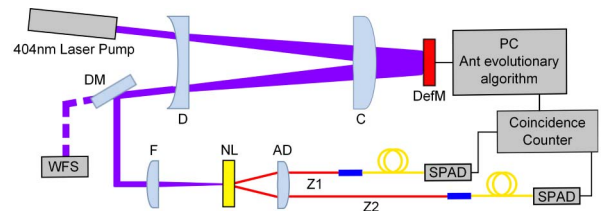


Fig. 1. (Color online) Experimental setup. The 404 nm laser passes through a Galilean telescope (lenses D and C , with $f_D = -250$ mm, $f_C = 500$ mm). After reflecting from the DefM, the beam is focused onto a NL by the lens F ($f_F = 287$ mm). A dichroic mirror (DM) sends 10% of the pump to a wavefront sensor (WFS) to its spatial shape evaluation. The 808 nm SPDC photons are collimated by an achromatic doublet (AD) ($f_{AD} = 75$ mm) and sent to fiber couplers (FC) after $Z_1 = 0.5$ m and $Z_2 = 2$ m of free space propagation. Finally, SPDC light is measured by two SPAD detectors and coincidences are evaluated with a coincidence counter. The outcome is utilized in a feedback loop with a DefM by Ant evolutionary algorithm.

is performed using a membrane DefM [8]. This device is an electrostatic-type DefM driven by 32 actuators arranged in a honeycomb pattern. The mirror has an aperture of 19 mm, with an active region of 11 mm. The pump beam has to match the DefM active region in order to fully exploit its capabilities. This is why a beam expander is used to double the pump beam diameter (2.5 mm of initial waist). After being reflected from the mirror, the beam is reduced by a second passage through the beam expander. This reverse path also provides the wavefront spatial frequencies amplification, thus enhancing the mirror action. The degenerate SPDC photon pairs at 808 nm are produced from the crystal. Each photon is coupled into a multimode fiber and sent to a high-efficiency single photon avalanche photodiode (SPAD). Two signals are combined on the coincidence counter.

As a starting point, the coincidence signal is maximized using a plane wavefront pump. To study the two-photon beam divergence, one multimode fiber is placed 2 m away from the crystal, while the other one is put 50 cm from the crystal to be used as a probe. Furthermore, two pinholes (2 mm diameter) are set along the longer path (Z_2) at a distance of 1.7 m from each to help with selecting a defined flight direction for evaluation.

The adaptive algorithm was selected to control the SPDC beam divergence over the path defined by pinholes. Among the vast choice of such algorithms [8], our choice was the Ant colony optimization [9] because of its small number of free parameters to set, which results in an easier calibration of the algorithm [10]. We employ the Ant colony optimization to demonstrate the enhancement of the collection efficiency of SPDC light and, therefore, to generate the SPDC beam with a diffraction-free characteristic by putting the DefM in a feedback loop with coincidence counts. Thus, mirror actuators are moved randomly by the algorithm and photon coincidences for each actuator configuration are measured. The target is to minimize this following quantity:

$$f(\text{coinc}) = N / \max(N, \text{coinc}), \quad (3)$$

where N stands for fixed lower coincidence counts bound and coincidences measured by SPADs are labeled with *coinc*; in addition $0 < f \leq 1$. N is chosen arbitrarily by the user and is usually set at half the initial signal. Minimizing Eq. (3) results in maximizing coincidence counts (this equation corresponds to the shortest path in the “traveling salesman problem” [11]). Each actuator configuration is associated to a quantity τ called trial. After setting an initial value of τ for the first patterns (equal to actuator number), the amount $\Delta\tau \propto 1/f$ is calculated and added to τ , thus updating trial intensity. Then new configurations are chosen with a probability proportional to τ , thus leading the algorithm to select patterns with the highest amount of trial. Consequently, mirror configurations which minimize f are achieved. In addition, when actuator configuration provides a value of f less than the previous, this value is stored and the mirror configuration is saved. Gradually, the algorithm explores new actuator patterns, refreshing the value of f each time a new minimum is achieved. The optimum configuration is reached following an exponential asymptotical growth as shown in Fig. 2.

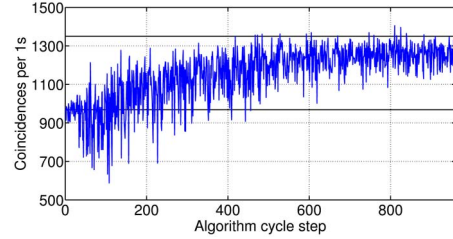


Fig. 2. (Color online) Coincidence evolution provided by the algorithm steps. Ant algorithm maximizes the coincidence counts as explained in the text. As a result, a pattern converging to an asymptotic value is achieved. Solid black lines illustrate the average values of initial and final coincidence counts measured over 60 s of exposure time.

Patterns providing a nearly flat wavefront are selected as initial conditions (initial 32 steps of Fig. 2). Consequently, we propose to start from a mirror configuration, which is not so far from the coincidence maximum, thus, avoiding any possible stagnation behavior [12]. In addition, starting from a good position allows us to speed up algorithm work. For instance, each measurement requires at least 1 s in order to achieve a signal-to-noise ratio less than 5%.

Several runs of the algorithm showed an increase in coincidences by almost 40%. This result means that the system is able to adapt SPDC beam size and divergence to match the path defined by the pinholes, thus improving the initial signal quality for this task. This optimization, resulting from a substantial alteration of the pump wavefront, is illustrated in Fig. 3. The optimized wavefront is studied in terms of its Zernike coefficient expansion. The most significant contribution is defocus, as expected. At the same time, the fiber coupling optimization is also influenced by higher-order terms, such as astigmatism $Z_{2,2}$ and coma (both $Z_{3,1}$ and $Z_{3,-1}$). The overall effect of these aberrations is shown in Fig. 4, which compares SPDC beam spot in front of the second pin-hole (at 1.5 m from the crystal), before (a) and after (b) the algorithm run.

This approach provides a substantial reduction of SPDC spot size during the free-space propagation, with the optimized spot being almost one-fifth of the initial spot size. As a result, the divergence of SPDC light beam has been corrected by artificial aberrations introduced by the adaptive optics elements in the pump beam.

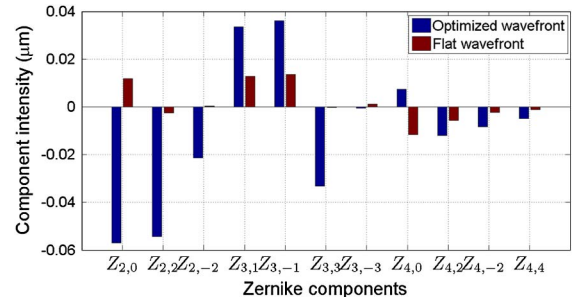


Fig. 3. (Color online) Measured low order Zernike components for each wavefront, before and after the optimization. In the case of flat wavefront (RMS = 0.01), all Zernike terms are less than 0.01 μm . The optimized wavefront exhibits a significant growth in both second and third order aberrations.

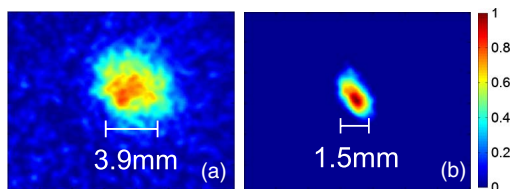


Fig. 4. (Color online) Comparison between SPDC beam spots at 1.5 m from the crystal, acquired with an image intensifier with nominal gain of 1000 and a low-noise CCD camera, with acquisition time of 60 s. The images correspond to (a) the flat wavefront (b) and the optimized case. A substantial reduction of beam diameter can be observed.

The beam size is now adapted to fit the pinhole diameter size. The shape of the spot also changes after the algorithm run. The optimized spot is no longer circular. It is stretched along the diagonal direction because of astigmatism and coma aberration. As a result, the SPDC beam optimization is the result of both defocus aberrations, which compensate SPDC beam divergence and higher order aberrations that contribute to the beam collimation over the long distance.

We tested the efficiency of the algorithm for controlling spacial parameters of the biphoton wave function using a challenging task of optimizing the coupling of the down converted radiation into single-mode fibers. The coincidence counts increase with the algorithm steps and are shown in Fig. 5. The coincidences in 60 s have been measured before and after the algorithm optimization. We obtained $20,780 \pm 144$ coincidences at the starting point, while we achieved $25,418 \pm 159$ by the optimization algorithm. The deformation of the mirror allows us to increase the coincidences by more than 20%.

In conclusion, we used a DefM for the laser pump radiation as an adaptive optics control for optimization of the two-photon wave-function spatial profile in the case of down-converted entangled photons. The optimized beam divergence of entangled photon pairs enables us to obtain diffraction-free propagation over significant distances (2 m) on the testbed. This result is achieved with an Ant evolutionary algorithm that works using feedback with the DefM. This approach is capable to find the best wavefront for centering SPDC light beams along a chosen direction, to optimize their spatial divergence, and to enhance the fiber coupling efficiency. The final wavefront imposed by the DefM includes both second- and

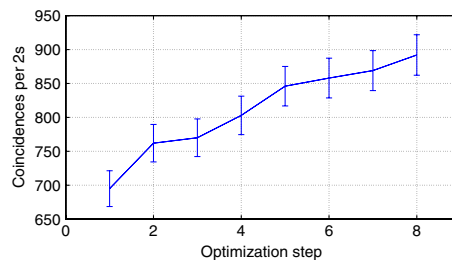


Fig. 5. (Color online) Coincidence evolution provided by algorithm for single-mode coupling (we only show the steps increasing the coincidences).

third-order aberrations (in addition to a possible tilt), to eliminate the biphoton beam divergence and aberrations.

We acknowledge Strategic-Research-Project QUIN-TET of the Department of Information Engineering and the Strategic-Research-Project QUANTUMFUTURE, both of the University of Padova.

References

1. A. V. Belinskii and D. N. Klyshko, *Zh. Eksp. Teor. Fiz.* **105**, 487 (1994).
2. T. B. Pittman, D. V. Strekalov, D. N. Klyshko, M. H. Rubin, A. V. Sergienko, and Y. H. Shih, *Phys. Rev. A* **53**, 2804 (1996).
3. C. H. Monken, P. H. Souto Ribeiro, and S. Padua, *Phys. Rev. A* **57**, 3123 (1998).
4. C. Bonato, S. Bonora, A. Chiuri, P. Mataloni, G. Milani, G. Vallone, and P. Villoresi, *J. Opt. Soc. Am. B* **27**, A175 (2010).
5. A. F. Abouraddy, P. R. Stone, A. V. Sergienko, B. E. A. Saleh, and M. C. Teich, *Phys. Rev. Lett.* **93**, 213903 (2004).
6. C. Bonato, A. V. Sergienko, B. E. A. Saleh, S. Bonora, and P. Villoresi, *Phys. Rev. Lett.* **101**, 233603 (2008).
7. P. Kolenderski, W. Wasilewski, and K. Banaszek, *Phys. Rev. A* **80**, 013811 (2009).
8. P. Villoresi, S. Bonora, M. Pascolini, L. Poletto, G. Tondello, C. Vozzi, M. Nisoli, G. Sansone, S. Stagira, and S. De Silvestri, *Opt. Lett.* **29**, 207 (2004).
9. E. Bonabeau, M. Dorigo, and G. Theraulaz, *Nature* **406**, 39 (2000).
10. S. Bonora, I. Capraro, L. Poletto, M. Romanin, C. Trestino, and P. Villoresi, *Rev. Sci. Instrum.* **77**, 093102 (2006).
11. M. Dorigo and M. L. Gambardella, *IEEE Trans. Evol. Comp.* **1**, 53 (1997).
12. M. Dorigo, V. Maniezzo, and A. Colomi, *IEEE Trans. Syst.* **26**, 29 (1996).